MATHEMATICAL BIOSCIENCES
AND ENGINEERING
Volume **5**, Number **4**, October **2008**

doi:10.3934/mbe.2008.5.729

pp. **729–741**

MODELING EVOLUTION AND PERSISTENCE OF NEUROLOGICAL VIRAL DISEASES IN WILD POPULATIONS

Dobromir T. Dimitrov

Fred Hutchinson Cancer Research Center,
1100 Fairview Ave N., LE-400, P.O. Box 19024, Seattle, WA 98109-1024 U.S.A.

Aaron A. King

Departments of Ecology and Evolutionary Biology and Mathematics, University of Michigan,
North University Avenue, Ann Arbor, MI 48109-1048 USA

Abstract. Viral infections are one of the leading source of mortality worldwide. The great majority of them circulate and persist in wild reservoirs and periodically spill over into humans or domestic animals. In the wild reservoirs, the progression of disease is frequently quite different from that in spillover hosts. We propose a mathematical treatment of the dynamics of viral infections in wild mammals using models with alternative outcomes. We develop and analyze compartmental epizootic models assuming permanent or temporary immunity of the individuals surviving infections and apply them to rabies in bats. We identify parameter relations that support the existing patterns in the viral ecology and estimate those parameters that are unattainable through direct measurement. We also investigate how the duration of the acquired immunity affects the disease and population dynamics.

1. **Introduction.** The last couple of decades have brought the realization that improved health care services and the development of new drugs and vaccines are insufficient to remove the threat of infectious diseases. Despite overly optimistic predictions, a variety of emerging and re-emerging infectious diseases, including HIV, SARS, Ebola, and drug-resistant tuberculosis, have spread in developed and developing countries alike, and viral infections remain a leading source of mortality worldwide [21, 18]. The majority of all human infections depend on animal reservoirs for their maintenance. An estimated 61% of the 1,415 species of infectious organisms known to be pathogenic in humans are transmitted by animals, for which the human represents a dead-end host [10]. Nearly half (49%) of all emerging viruses cause encephalitis or serious neurological clinical symptoms with 80% of neurotropic viruses being zoonotic [19].

The majority of mathematical models used to investigate viral infections in wildlife are variants on the traditional SEIR framework long used to describe disease dynamics in humans and domestic animals [13, 2]. These models follow the progression of a stereotypical infection from the moment of viral transmission through latent and infectious periods and ultimately to recovery or death of the host. Such models provide a relatively simple environment for theoretical analysis of disease

2000 *Mathematics Subject Classification.* Primary: 92D30; Secondary: 37N25.
Key words and phrases. epizootic models; zoonotic infection; rabies; bats.
This project is supported by NSF/NIH-EID Grant 043041.

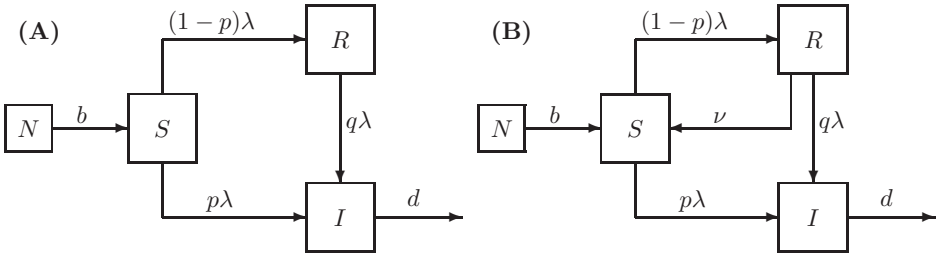

FIGURE 1. Diagrams of epizootic models with permanent and temporary immunity. The force of infection is $\lambda = \beta I/N$.

evolution and a good interface with clinical data including case histories, vaccination, and treatment records, etc. These data are frequently available in the case of human diseases for which early symptoms can be identified and recorded. They are also collectible for some livestock diseases, where surveillance and control of host populations is sometimes feasible. Comparable data are not so readily available in the case of diseases of wild fauna. In a wild context, it is often practically impossible to distinguish different phases of a disease's progression by direct observation. Trackability of individual animals by recapture varies from difficult in the case of foxes and raccoons to infeasible in the case of numerous and highly gregarious bats and rodents. However, snapshot field data can be used to estimate prevalence of active viral infections and of titers of virus-specific antibodies (which indicate past exposure to virus) in wild populations. Moreover, experimental infection studies can be used to assess individual susceptibility [12]. Such studies confirm that exposure to virus need not result in symptomatic infection but may rather produce a subclinical response with immune system activation and consequent protection from reinfection.

In this paper we propose models that capture the nonstereotypical nature of viral exposures. In these models, the course of infection can follow alternative pathways leading either to infectiousness or immunization. These models provide an interface with existing snapshot data and allow us to analyze the potential role of passive infection in the persistence of disease in the population. The paper is organized as follows. In Section 2 we formulate and analyze models that assume permanent and temporary protection in the immunized class. In Section 3 we apply our analysis to the case of rabies in bats, which accounts for about 90% of indigenous human rabies cases in U.S. [9, 17]. We determine regions in the parameter space consistent with observations on bat rabies [22, 8]. We also investigate the effect of the duration of infection-derived immunity on disease progression in a bat population. We use the final section to discuss some future research directions.

2. **Model formulation and analysis.**

We formulate and analyze models of disease dynamics under two distinct assumptions: 1) surviving hosts develop lifelong immunity (Fig. 1A) and 2) they develop immunity that wanes in time (Fig. 1B).

Each model divides the host population into three classes: susceptible (S), infected (I), and immunized (R). Contacts between susceptible and infected individuals result in flows from the susceptible class to the other two classes. When

exposed, susceptible hosts become actively infectious with probability p. The infection is assumed lethal: infected hosts ultimately die of the disease. An additional flow allows individuals in the immunized class, upon re-exposure, to enter the infectious class. The relative susceptibility parameter q governs this flow and therefore measures the efficacy of acquired immunity. In the model with temporary immunity (MTI), protection wanes at rate ν; i.e., the average duration of immunity is $1/\nu$.

The model with permanent immunity (MPI) is expressed by the following system:

$$\begin{aligned}
\tfrac{dS}{dt} &= bN - \beta\tfrac{SI}{N} - mS \\
\tfrac{dI}{dt} &= p\beta\tfrac{SI}{N} + q\beta\tfrac{RI}{N} - (m+d)I \\
\tfrac{dR}{dt} &= (1-p)\beta\tfrac{SI}{N} - q\beta\tfrac{RI}{N} - mR
\end{aligned} \tag{1}$$

where $N = S + I + R$ is the total population size, b and β stand for the birth rate and the effective contact rate, respectively, m is the natural loss rate due to death and dispersal, and d is the disease-related death rate.

The model with temporary immunity (MTI) is defined by the following system:

$$\begin{aligned}
\tfrac{dS}{dt} &= bN + \nu R - \beta\tfrac{SI}{N} - mS \\
\tfrac{dI}{dt} &= p\beta\tfrac{SI}{N} + q\beta\tfrac{RI}{N} - (m+d)I \\
\tfrac{dR}{dt} &= (1-p)\beta\tfrac{SI}{N} - q\beta\tfrac{RI}{N} - (m+\nu)R.
\end{aligned} \tag{2}$$

In the absence of infection, systems (1) and (2) reduce to the single equation $\frac{dS}{dt} = (b-m)\,S$, justifying the assumption $b > m$. We assume also that acquired partial immunity decreases susceptibility, i.e., $p > q$.

To analyze systems (1) and (2) we reformulate them in terms of the fractions of the population in each class. Accordingly, let $s = S/N$, $i = I/N$, $r = R/N$ denote the fractions of the host population in each state. Then (1) becomes

$$\begin{aligned}
\frac{ds}{dt} &= b\,(1-s) + (d-\beta)\,s\,i \\
\frac{di}{dt} &= (p-q)\,\beta\,s\,i + (d - q\,\beta)\,i^2 + (q\,\beta - b - d)\,i \\
\frac{dN}{dt} &= (b - m - d\,i)\,N,
\end{aligned} \tag{3}$$

while (2) becomes

$$\begin{aligned}
\frac{ds}{dt} &= b\,(1-s) + \nu\,(1-s-i) + (d-\beta)\,s\,i \\
\frac{di}{dt} &= (p-q)\,\beta\,s\,i + (d - q\,\beta)\,i^2 + (q\,\beta - b - d)\,i \\
\frac{dN}{dt} &= (b - m - d\,i)\,N.
\end{aligned} \tag{4}$$

Note that, in both cases, the first two equations are decoupled from the third.

We analyze the dynamics of the resulting fractional models (3) and (4) in the region of the si-plane that contains all feasible trajectories:

$$\mathcal{R} = \{(s,i) : s \geq 0, i \geq 0, s+i \leq 1\}. \tag{5}$$

For this region the following theorem holds.

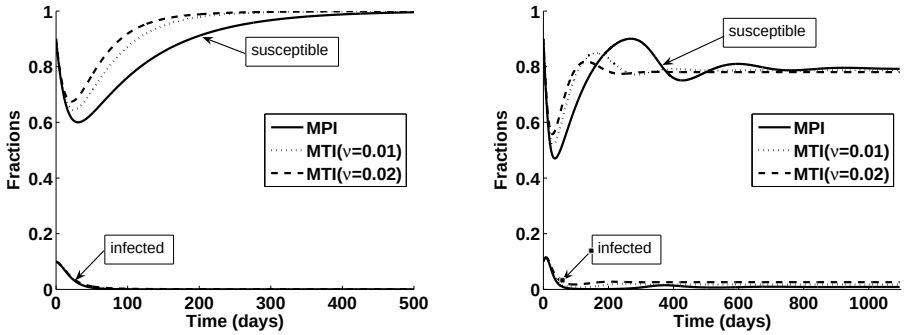

(a) $p = 0.4$, $s(0) = 0.9$, $i(0) = 0.1$ (b) $p = 0.5$, $s(0) = 0.9$, $i(0) = 0.1$

FIGURE 2. Dynamics of the fractional models with $b = 0.01$, $\beta = 0.5$, $d = 0.2$, $q = 0.1$.

Theorem 2.1. *The region $\mathcal{R}$ is forward invariant under systems (3) and (4).*

Proof. We evaluate the vector field defined by systems (3) and (4) on the boundary of the region $\mathcal{R}$. When $s = 0$ we have $\frac{ds}{dt} = b > 0$ and $\frac{ds}{dt} = b + \nu(1 - i) > 0$, respectively, while $\frac{di}{dt} = 0$ for both systems when $i = 0$. Therefore, all solutions starting in the first quadrant remain there. Along the line segment $s + i = 1$ the inequality $\frac{d(s+i)}{dt} = -(1-p)\beta i(1-i) \leq 0$ holds for both systems. Thus all solutions that start in $\mathcal{R}$ remain in $\mathcal{R}$. □

The global behavior of the fractional models in the region $\mathcal{R}$ is summarized as follows.

Theorem 2.2. *If $R_0 = \frac{p\beta}{b+d} < 1$ systems (3) and (4) both have a unique disease-free equilibrium, $s = 1$, $i = 0$, which is globally stable in $\mathcal{R}$. If $R_0 > 1$ then the disease-free equilibrium of each system is unstable and an unique stable enzootic equilibrium appears. The enzootic equilibria (s^*_{pi}, i^*_{pi}) and (s^*_{ti}, i^*_{ti}) of system (3) and system (4) for concurrent sets of parameters satisfy the inequality $i^*_{ti} > i^*_{pi}$.*

The proof of Theorem 2.2 is in Appendix A. The dependence on the basic reproductive number R_0 is unsurprising. The relation between enzootic equilibria of systems (3) and (4) predicts that with waning immunity the enzootic profile of the host population will stabilize at a relatively larger infectious fraction. As we will show, this affects the host population's chance of overcoming the infection. The simulations in Figure 2 show typical trajectories of the models under the two major dynamical scenarios.

Theorem 2.2 helps us to analyze the epizootic dynamics of MPI (1) and MTI (2) and to classify the possible dynamical scenarios that arise from an exposure to a viral infection. Our major goal is to determine conditions on the models' parameters leading to outcomes that are distinguishable using field data. We concentrate our attention on parameters such as the transmission rate (β) and susceptibilities (p and q) that are not directly measurable but might be estimated indirectly using the models. The remaining parameters (b, m and d) are estimable on the basis of experimental data (see below).

Models (1) and (2) predict three possible dynamical outcomes for a population exposed to a viral infection (Fig.3). An **endangered population** (Fig.3a) is driven

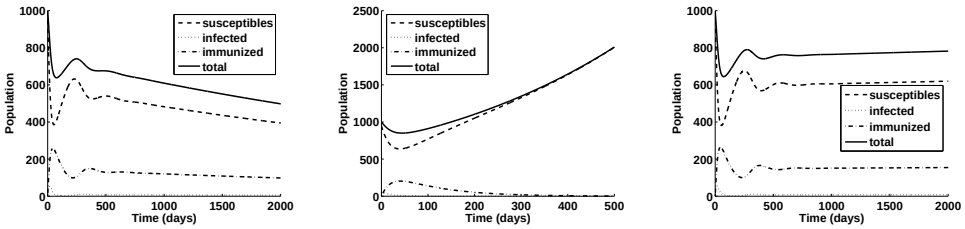

(a) Endangered population (b) Recovering population (c) Reservoir population

FIGURE 3. Population dynamics predicted by MPI and MTI.

to extinction by the disease and steadily declines in time. A **recovering population** (Fig.3b) is able to eradicate the disease, i.e., it asymptotically tends to a "naive" population. A **reservoir population** (Fig.3c) survives and grows in time. It continues to carry nonzero fractions of infected and immunized hosts.

The following theorem summarizes the conditions for MPI and MTI that lead to each of the outcomes above:

Theorem 2.3. *If the susceptibility of naive hosts is low ($p < \frac{b+d}{\beta}$), then $R_0 < 1$ and the population overcomes and clears the disease regardless of the properties of the acquired immunity. Conversely, if the susceptibility (p) is high, then the fate of the population is decided by i^*, the fraction of hosts infected at equilibrium in systems (3) or (4). In particular, if $i^* > \frac{b-m}{d}$ the disease leads the population to extinction. Otherwise, the population survives the disease and its epizootic profile approaches a fractional distribution described by (s^*, i^*).*

The results of Theorem 2.3 imply that the persistence of the pathogen in the host population is assured only when two independent parameter conditions are simultaneously satisfied. The "enzootic condition" ($R_0 > 1$) is required for the disease to persist; the "survival condition" ($i^* < \frac{b-m}{d}$) ensures that the host population will persist. Limiting the duration of acquired immunity increases the infected fraction, i^*, of the population and can therefore lead to failure of the survival condition; i.e., to extinction of the host population.

3. **Application to rabies in bats.** The MPI and MTI models are motivated by the phenomenology of rabies in bats, particularly in Brazilian free-tailed bats (*Tadarida brasiliensis*). Separate studies [22, 8] show seroprevalence in 40%–75% of apparently healthy Brazilian free-tailed bats tested in unbiased surveys. The same surveys also showed little evidence of active infection, with 0–1% of the bats tested having virus in brain tissue, or viral RNA in salivary swabs, when brain could not be tested. Field data [22, 23] supported by laboratory studies [3, 12] demonstrate that bats exposed to the viruses often develop antibodies and clear peripheral infections without developing clinical signs of disease, suggesting, perhaps, that it is animals with suppressed immune response that develop and succumb to rabies infections. Brazilian free-tailed bats live in huge colonies in caves and under bridges. Their dense aggregation and constant biting and grooming suggest potentially high contact rates, but it has proved impossible to measure contact rates directly. Even if it were possible to measure raw contact rates, it would be difficult to estimate what proportion of those contacts result in viral transmission and still harder to quantify the proportion of transmissions that lead to clinical

rabies. The parameters β, p, and q of the MPI and MTI models regulate these proportions and are therefore the main subject of our investigation. The remaining parameters can be estimated on the basis of previous field and experimental studies [8, 22]. The birth rate, b, range of 0.0009–0.0011 da^{-1} is based on the assumption of equal sex ratio and the fact that most female bats ($> 80\%$) give birth to a single offspring per year. The natural loss rate, m, is estimated to take values in the range 0.0008–0.001 da^{-1} in correspondence with the life expectancy of *T. brasiliensis* [14]. The realistic range for the disease-related mortality, d, (0.02–0.05 da^{-1}) is determined by the average lifespan of experimentally infected bats (20–50 da) [12]. In the following, we identify combinations of the parameters p, q, and β that support the observed disease dynamics.

We first investigate how the susceptibilities p and q, independently and in combination, influence bat rabies dynamics. Since the susceptibility of naive bats, p, enters R_0, it mediates the switch from epizootic to enzootic behavior when increased. On the other hand, an increase in either p or q results in a decline of the equilibrium susceptible fraction, s^*, and an increase in the equilibrium infected fraction, i^*. Therefore, the survival condition will be violated for sufficiently high values of p and/or q. Figure 4 presents the regions in the qp-plane corresponding to the dynamics predicted in Theorem 2.3. Below the enzootic boundary $p = \frac{b+d}{\beta}$ the virus dies out. To the right of the survival boundary

$$p = \frac{(b-m)\,(d\,(d+m)+\beta\,(b-d-m)}{d\,(b\,d-(b-d-m)\,\nu)}\,q + \frac{(d+m)\,((d+\nu)\,m+(b-m)\,\beta)}{\beta\,(b\,d-(b-d-m)\,\nu)},$$

the host population dies out. The remaining triangular region contains all combinations of p and q that ensure persistence of the disease in a vital host population. Figures 4a and 4b show this feasible region for MPI at two levels of the effective contact rate, β. Note that the feasible region in these two cases impose tight limitations on the susceptibilities p and q; these restrictions grow sharper as background mortality, m, increases (Fig. 4b). The third diagram (Fig. 4c) compares the feasible region for MPI to that of MTI with various durations of immune protection. Experimental infections suggest that bats surviving infection lose their antibody titer after a period of six to twelve months following inoculation [12]. However, they seem to have an immune protection for a longer period. The parameter values for ν used here correspond to protection periods of one year ($\nu = 0.027$ da^{-1}) and two years ($\nu = 0.014$ da^{-1}). Varying ν does not influence the ability of the rabies infection to invade the colony; it does strongly affect the host colony's ability to persist in the presence of the disease. The influence of a time-limited immunity protection on the parameter regions is almost identical to that of increased background mortality; i.e, of decreased life expectancy. With rapidly waning immunity, the region of parameter space corresponding to bat-rabies coexistence becomes very narrow. Under such circumstances, immunosuppression events due to adverse weather, food scarcity, or environmental change might easily lead to host-population decline and extinction. All available evidence suggests, however, that despite the widespread presence of rabies in bats, massive die-offs are uncommon [20]. Thus, our analysis provides support for the hypothesis of long-lasting immunity against rabies. Further support for this hypothesis is obtained from the fact the most bats that survive experimental rabies infections do not succumb after consecutive exposures to high viral concentrations even when the re-exposures are conducted long after the initial inoculation [12].

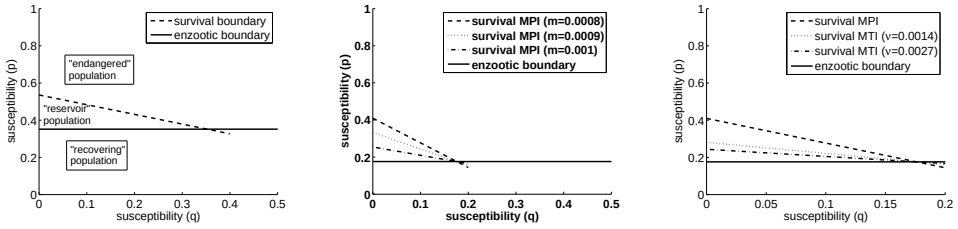

(a) $\beta = 0.06, m = 0.0008$ (b) $\beta = 0.12$ (c) $\beta = 0.12, m = 0.0008$

FIGURE 4. Feasible regions in the plane of susceptibilities q, p with $b = 0.0011$, $d = 0.02$ and various contact rates, background mortality, and durations of immunity.

We next consider completely effective immunity ($q = 0$) that mirrors the experimental data cited above. We focus our attention on the effective contact rate, β. Again, experimental measurements are unavailable. Figure 5 shows the regions in the βp-plane corresponding to each of the three dynamical alternatives described in Theorem 2.3 at each of two levels of disease-related mortality, d. The enzootic boundary in those simulations is given by $p = \frac{b+d}{\beta}$; the survival boundary is

$$p = \frac{(b-m)(d+m)}{b\,d-(b-d-m)\,\nu} + \frac{d\,(d+m)\,(m+\nu)}{b\,d-(b-d-m)\,\nu}\,\frac{1}{\beta}.$$

The shape and the size of the feasible region is not affected significantly by the mortality rate. This allows us to draw some conclusions about the levels of susceptibility and effective contacts in real bat colonies. The range of susceptibility that supports infection without collapsing the bat population (5%–40%) suggests that the majority of exposures result in development of immunity rather than disease and death. This contrasts sharply with the situation in mammalian carnivores, in which susceptibility rates are estimated at over 90% [2, 4]. Not surprisingly, rabies epizootics in carnivores often have a major impact on local populations. The effective contact rate β must be sufficiently large ($\beta > d + b$) for the host population to be able to support a persistent infection (see the proof of Theorem 2.2). Figure 5 suggests that each infected bat should, on average, successfully transfer rabies at least once per 10 days to keep the virus circulating in the colony. Experimentally infected bats vary in infectiousness during the period before they succumb to rabies. In light of this, our results predict that contact rates in natural populations should be higher.

Loss of immunity restricts the feasible range of p significantly (Fig. 5c). For example, if the average duration of immunity is one year ($\nu = 0.0027$ da^{-1}), then $p > 20\%$ leads to host population extinction. In other words, our results show that if immunity wanes, a combination of low susceptibility and high contact rates are needed for the feasibility of enzootic rabies in bats. This scenario corresponds to the hypothesis that the high seroprevalence in colonial bats is the result of frequent exposure of individuals to small viral inocula that give rise to short-lived immunity.

4. **Discussion.** In this paper we examined epizootic models that allow for alternative courses of infection: exposure to pathogen can lead either to infectiousness accompanied by lethal disease or to longer- or shorter-lived immunity. These models may be useful descriptions of viral neurological infections such as rabies in wild

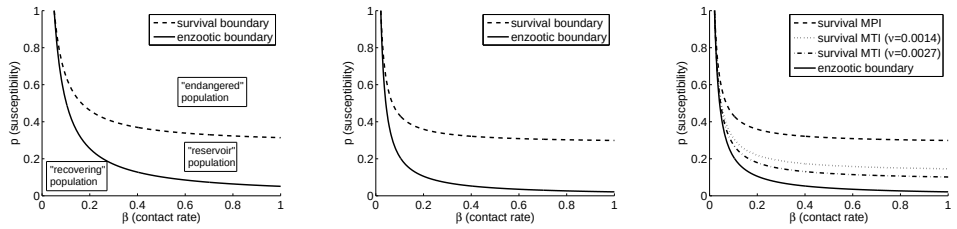

(a) $d = 0.05$ (b) $d = 0.02$ (c) $d = 0.02$

FIGURE 5. Feasible regions in the βp-parameter plane with different levels of disease-related mortality and immunity protection.

mammals because the progress of these infections often depends on the size of the inoculum. That is, the fate of the exposed individual may usefully be thought of as being decided at the time of exposure.

The models proposed interface well with existing field data on prevalence and seroprevalence, interpreted as indicators of infectious and immunized population fractions, respectively. Analysis of the models reveals three possible dynamical outcomes: 1) the population is able to clear the virus; 2) the population is driven to extinction by the disease; and 3) long-term coexistence of virus and host. In the latter case, the wild population can act as a pathogen reservoir and therefore a source of risk to humans and domestic animals. Two conditions, epizootic and survival, on the model parameters must be satisfied for such a reservoir to exist. These conditions can be used to determine ranges for some unmeasurable parameters that are consistent with the observation of persistence of rabies in colonies of Brazilian free-tailed bats. Examination of feasibility regions in the susceptibility and effective contact rate parameters suggest an explanation for the different phenomenology of rabies in bats compared to mammalian carnivores.

We are currently working on a modeling approach that incorporates a "carrier" state of infectious but asymptomatic animals. The existence of such a state in bats has been tested repeatedly but has not to date been corroborated in experimental studies using several bat species and different lyssaviruses [3, 7, 6, 5, 11, 15]. Some support for the carrier-state hypothesis is provided by a recent report of experimentally infected vampire bats shedding virus in saliva without evidence of virus in brain tissue [1]. These results should be interpreted cautiously because several aspects of the study are inconsistent [16]. Our goal is to use simple models to delineate the parameter regimes consistent with existing experimental data. The generality of the modeling approach exemplified here makes it applicable to different viral infections in bats and other wild mammals. Our analysis emphasizes the importance of considering alternative outcomes to viral exposure. Such effects have been overlooked in the traditional SEIR framework and are likely to be a fruitful subject for future investigation.

5. **Acknowledgments.** This work is dedicated to Dr. Thomas G. Hallam on his 70th birthday.

The authors thank anonymous referees for the useful comments on an earlier draft.

REFERENCES

[1] A. Aguilar-Setien, E. Loza-Rubio, M. Salas-Rojas, N. Brisseau, F. Cliquet, P. P. Pastoret, S. Rojas-Dotor, and E. Tesoro. Salivary excretion of rabies virus by healthy vampire bats. *Epidemiology and Infection*, 133(3):517–522, 2005.

[2] R. M. Anderson, H. C. Jackson, R. M. May, and A. M. Smith. Population-dynamics of fox rabies in Europe. *Nature*, 289 (5800):765–771, 1981.

[3] G. M. Baer and G. L. Bales. Experimental rabies infection in the Mexican freetail bat. *Journal of Infectious Diseases*, 117:82–90, 1967.

[4] J. E. Childs, A. T. Curns, M. E. Dey, L. A. Real, L. Feinstein, O. N. Bjornstad, and J. W. Krebs. Predicting the local dynamics of epizootic rabies among raccoons in the United States. *Proceedings of the National Academy of Sciences of the United States of America*, 97(25):13666–13671, 2000.

[5] D. G. Constantine. Transmission experiments with bat rabies isolates: bite transmission of rabies to foxes and coyote by free-tailed bats. *Am J Vet Res*, 27:20–23, 1966.

[6] D. G. Constantine. Transmission experiments with bat rabies isolates: reaction of certain carnivora, opossum, and bats to intramuscular inoculations of rabies virus isolates from free-tailed bats. *Am J Vet Res*, 27:16–19, 1966.

[7] D. G. Constantine. Transmission experiments with bat rabies isolates: responses of certain carnivora to rabies virus isolated from animals infected by nonbite route. *Am J Vet Res*, 27:13–15, 1966.

[8] D. G. Constantine, E. S. Tierkel, M. D. Kleckner, and D. M. Hawkings. Rabies in New Mexico cavern bats. *Public Health Reports*, 83:303–316, 1968.

[9] R. V. Gibbons, R. C. Holman, S. R. Mosberg, and C. E. Rupprecht. Knowledge of bat rabies and human exposure among United States cavers. *Emerg Infect Dis*, 8:532–534, 2002.

[10] J. L. Heeney. Zoonotic viral diseases and the frontier of early diagnosis, control and prevention. *Journal of Internal Medicine*, 260(5):399–408, 2006.

[11] G. J. Hughes, I. V. Kuzmin, A. Schmitz, J. Blanton, J. Manangan, S. Murphy, and C. E. Rupprecht. Experimental infection of big brown bats (Eptesicus fuscus) with Eurasian bat lyssaviruses. *Arch Virol*, 151:20212035, 2006.

[12] F. R. Jackson, A. S. Turmelle, D. M. Farino, R. Franka, G. F. McCracken, and C. E. Rupprecht. Experimental rabies virus infection of big brown bats (Eptesicus fuscus). *Journal of Wildlife Diseases, accepted*, 2008.

[13] W. O. Kermack and McKendrick. A. G. A contribution to the mathematical theory of epidemics. *Proc. Roy. Soc. A*, 115:700721, 1927.

[14] T. H. Kunz and S. K. Robson. Postnatal-growth and development in the Mexican free-tailed bat (Tadarida-Brasiliensis-Mexicana) - birth size, growth-rates, and age estimation. *Journal of Mammalogy*, 76 (3):769–783, 1995.

[15] I. V. Kuzmin and A. D. Botvinkin. The behaviour of bats Pipistrellus pipistrellus after experimental inoculation with rabies and rabies-like viruses and some aspects of pathogenesis. *Myotis*, 34:93–99, 1996.

[16] I. V. Kuzmin and C. E. Rupprecht. Bat rabies. In A.C. Jackson and W.H. Wunner, editors, *Rabies, 2nd edition*, pages pp. 259–308. Acad Press, 2007.

[17] S. L. Messenger, J. S. Smith, and C. E. Rupprecht. Emerging epidemiology of bat-associated cryptic cases of rabies in humans in the United States. *Clinical Infectious Diseases*, 35 (6):738–747, 2002.

[18] D. M. Morens, G. K. Folkers, and A. S. Fauci. The challenge of emerging and re-emerging infectious diseases. *Nature*, 430(6996):242–249, 2004.

[19] K. J. Olival and P. Daszak. The ecology of emerging neurotropic viruses. *Journal of Neurovirology*, 11(5):441–446, 2005.

[20] M. J. Pybus, D. P. Hobson, and D. K. Onderka. Mass mortality of bats due to probable blue-green algal toxicity. *Journal of Wildlife Diseases*, 22:449–450, 1986.

[21] S. J. Schrag and P. Wiener. Emerging infectious disease: What are the relative roles of ecology and evolution. *Trends in Ecology & Evolution*, 10(8):319–324, 1995.

[22] R. Steece and J. S. Altenbach. Prevalence of rabies specific antibodies in the Mexican free-tailed bat (Tadarida brasiliensis mexicana) at Lava Cave, New Mexico. *Journal of Wildlife Diseases*, 25:490–496, 1989.

[23] C. V. Trimarchi and J. G. Debbie. Naturally occurring rabies virus and neutralizing antibody in 2 species of insectivorous bats of New York State. *Journal of Wildlife Diseases*, 13(4):366–369, 1977.

Appendix A. **Proof of Theorem 2.2.** Solving the equilibrium conditions of systems (3) and (4) leads to the existence of a common disease-free equilibrium ($s = 1, i = 0$) and up to two enzootic equilibria for each system. When $q \neq \frac{d}{\beta}$, each enzootic equilibrium (s^*_{pi}, i^*_{pi}) of system (3) satisfies $i^*_{pi} = g(s^*_{pi})$ where $g(s) = 1 + \frac{b-(p-q)\beta s}{d-q\beta}$ and s^*_{pi} is a root of

$$\begin{aligned} f_{pi}(s) &= (d-\beta)g(s)s + b(1-s) = \\ &= -\tfrac{(p-q)\beta(d-\beta)}{d-q\beta}s^2 + \left((d-\beta)(1+\tfrac{b}{d-q\beta}) - b\right)s + b \end{aligned} \tag{6}$$

while an enzootic equilibrium (s^*_{ti}, i^*_{ti}) of system (4) satisfies $i^*_{ti} = g(s^*_{ti})$ where s^*_{ti} is a root of

$f_{ti}(s) = -\frac{(p-q)\beta(d-\beta)}{d-q\beta}s^2 + \left((d-\beta)(1+\frac{b}{d-q\beta}) - \frac{\nu(d-p\beta)}{d-q\beta} - b\right)s + b - \frac{b\nu}{d-q\beta}$.

The proof of Theorem 2.2 is based on a standard stability analysis of the existing equilibria. The conclusions for the dynamics of both systems at each analytical step overlap. Therefore we provide the proof for the MPI system only since the case of MTI is quite similar though it is computationally more challenging. The proof consist of three major parts: 1) establishing an uniqueness of the enzootic equilibrium in $\mathcal{R}$; 2) analysis of the local stability of the existing equilibria; and 3) analysis of the global dynamics of system (3) formulated in the following propositions. Let $A = -\frac{(p-q)\beta(d-\beta)}{d-q\beta}$, $B = (d-\beta)(1+\frac{b}{d-q\beta}) - b$, and $C = b$ are the coefficients of $f_{pi}(s)$. Note that $C > 0$ and thus if $A < 0$ there is a unique positive root of $f_{pi}(s) = 0$.

Proposition 1. *If $R_0 = \frac{p\beta}{b+d} < 1$ then system (3) has no enzootic equilibria. If $R_0 > 1$ a unique interior equilibrium exists in $\mathcal{R}$.*

Proof. We consider the following cases:

- If $\beta < d$ then $A < 0$ and the function $f_{pi}(s)$ has a unique positive root s^*. It is less then 1 exactly when $f(1) < 0$, which is equivalent to $g(1) < 0$. However, since $q < p \leq 1$, $\beta < d$ implies $R_0 < 1$ and $g(1) = \frac{d+b}{d-q\beta}(1-R_0) > 0$. Therefore, there are no enzootic equilibria in $\mathcal{R}$;
- If $\beta = d$ the only positive root of $f_{pi}(s) = 0$ is $s^* = 1$, which leads us to the disease free equilibrium;
- If $d < \beta \leq b+d$ the nonlinear isocline of System (3) lies below the line $i+s = 1$ only for values of s between $s_{iso} = \frac{b}{\beta-d}$ and $s = 1$ (see Fig.6-a). Since in this case $s_{iso} > 1$ the nonlinear isocline does not intersect $\mathcal{R}$ and therefore there are no equilibria inside $\mathcal{R}$.
- If $\beta > b+d$ and $q > \frac{d}{\beta}$ then $A < 0$ and $f_{pi}(s)$ has a unique positive root s^*. Since $f_{pi}(0) = C > 0$ the following equivalence holds:

  $$s^* < 1 \iff g(1) > 0 \iff R_0 > 1.$$

  Then an equilibrium $(s^*, g(s^*))$ exists in $\mathcal{R}$ only if $R_0 > 1$ and also $0 < g(s^*) + s^* < 1$. The latter inequality leads to $s^* > s_{iso}$ (see Fig.6-b), which is equivalent to $f_{pi}(s_{iso}) > 0$. After some calculations it can be showed that

  $$f_{pi}(s_{iso}) = \frac{(1-p)b^2\beta}{(q\beta-d)(\beta-d)} > 0$$

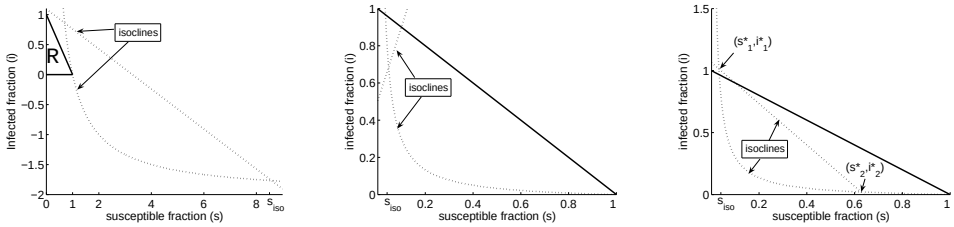

(a) $d < \beta < b + d$ (b) $\beta > b + d$, $q > \frac{d}{\beta}$ (c) $\beta > b + d$, $q < \frac{d}{\beta}$

FIGURE 6. Isoclines configurations for MPI

Therefore (s^*, i^*) belongs to $\mathcal{R}$ provided that $R_0 > 1$;

- If $\beta > b+d$ and $q = \frac{d}{\beta}$ a unique nontrivial equilibrium $\left(s^* = \frac{b}{p\beta - d}, i^* = \frac{p\beta - d - b}{\beta - d}\right)$ exists and it belongs to $\mathcal{R}$ if and only if $R_0 > 1$.
- If $\beta > b + d$ and $q < \frac{d}{\beta}$ then $A > 0$ and $f_{pi}(s)$ has either zero or two positive roots. Evaluations $f_{pi}(0) > 0$ and $f_{pi}(s_{iso}) < 0$ imply that $f_{pi}(s)$ has exactly two positive roots that satisfy $0 < s_1^* < s_{iso} < s_2^*$ (see Fig.6-c). The nonlinear isocline of System (3) lies in $\mathcal{R}$ only for values of s between $s = s_{iso}$ and $s = 1$ and therefore $(s_1^*, g(s_1^*)) \notin \mathcal{R}$. Moreover, $(s_2^*, g(s_2^*)) \in \mathcal{R}$ only if $s_2^* < 1$. The latter inequality is satisfied if and only if $g(1) < 0$, which in turn is equivalent to $R_0 > 1$. Therefore, the system (3) has a unique equilibrium in $\mathcal{R}$ if and only if $R_0 > 1$ while $R_0 < 1$ implies that there is no equilibrium in $\mathcal{R}$. □

The local stability of each equilibrium depends on the eigenvalues of the Jacobian matrix of system (3) given by

$$J(s,i) = \begin{pmatrix} -(\beta - d)i - b & -(\beta - d)s \\ (p-q)\beta i & (p-q)\beta s + 2(d - q\beta)i - (b + d - q\beta) \end{pmatrix}. \tag{7}$$

Proposition 2. *The disease free equilibrium* $(1, 0)$ *of system (3) is locally asymptotically stable node if* $R_0 < 1$ *and unstable (saddle point) otherwise.*

Proof.

$$J(1,0) = \begin{pmatrix} -b & -(\beta - d) \\ 0 & p\beta - b - d \end{pmatrix}. \tag{8}$$

Therefore the equilibrium $(1, 0)$ is locally asymptotically stable node if $R_0 = \frac{p\beta}{b+d} < 1$ and unstable (saddle point) otherwise. □

Proposition 3. *When it exists, the enzootic equilibrium* (s^*, i^*) *of system (3) is locally asymptotically stable.*

Proof. The Jacobian matrix $J(s^*, i^*)$ can be put into the form:

$$J(s^*, i^*) = \begin{pmatrix} -\frac{b}{s^*} & -\frac{b(1-s^*)}{i^*} \\ (p-q)\beta i^* & (d - q\beta)i^* \end{pmatrix}. \tag{9}$$

If $q > \frac{d}{\beta}$ then $Tr(J(s^*, i^*)) = -\frac{b}{s^*} - (q\beta - d)i^* < 0$ and $det(J(s^*, i^*)) = \frac{b(q\beta - d)i^*}{s^*} + (p - q)b\beta(1 - s^*) > 0$. Therefore (s^*, i^*) is locally asymptotically stable.

On the other hand, it is easy to see that when $q < \frac{d}{\beta}$ then $i^* < \frac{b}{d - q\beta}$. In particular, the proof of Proposition 1 shows that in this case $f_{pi}(s)$ has exactly two positive roots $s_1^* < s_2^*$ and $f_{pi}(s)$ takes negative values only between those roots (Fig.6-c). It is shown there also that s^* coincides with s_2^*. Consider the point

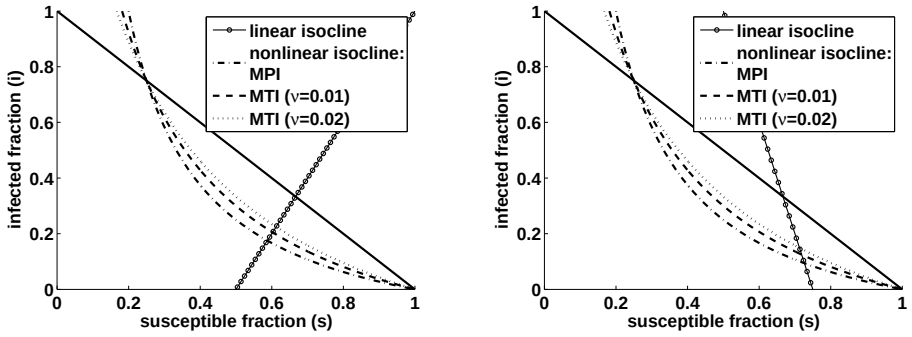

(a) $\beta > b + d$, $q > \frac{d}{\beta}$ (b) $\beta > b + d$, $q < \frac{d}{\beta}$

FIGURE 7. Effects of a time-limited immunity protection on the enzootic equilibrium.

$\left(\frac{d-q\beta}{(p-q)\beta}, \frac{b}{d-q\beta}\right)$, which, like (s^*, i^*), lies on the linear isocline of System (3). Since $f_{pi}\left(\frac{d-q\beta}{(p-q)\beta}\right) < 0$ it follows that $s^* > \frac{d-q\beta}{(p-q)\beta}$. The linear isocline has a negative slope, which implies that $i^* < \frac{b}{d-q\beta}$.

It follows that when $q < \frac{d}{\beta}$, $Tr(J(s^*, i^*)) = -b + (2d - \beta - q\beta)i^* < 0$. Moreover,

$$\begin{aligned} det(J(s^*, i^*)) &= -\frac{b(d-q\beta)i^*}{s^*} + (p-q)b\beta(1-s^*) \\ &> \frac{b}{s^*}((q\beta - d)i^* + (p-q)\beta i^* s^*) \\ &= -\frac{bi^*}{s^*}((d-q\beta)i^* - b) > 0. \end{aligned}$$

which complete the proof in this case. □

The global stability of the disease free equilibrium when $R_0 < 1$ is a direct implication of the Poincare-Bendixson Theorem. To conclude the proof of Theorem 2.2 we have to establish the relationships between the enzootic equilibria of systems (3) and (4). Variation in ν preserves the linear isocline of system (4). It also preserves the intersects of the nonlinear isocline with the line $x + y = 1$. An increase in ν leads to an increase in i^*_{ti} (see Fig.7). Since system (3) is a special case of systems (4) with $\nu = 0$ he relationships between the enzootic equilibria of the systems hold.

Finally, we address the global stability of the enzootic equilibrium.

Proposition 4. *System (3) has no periodic solutions in $\mathcal{R}$ for $q > \frac{d}{\beta}$.*

Proof. Define

$$L(s,i) = \frac{\partial}{\partial s}\left(H(s,i)F(s,i)\right) + \frac{\partial}{\partial i}\left(H(s,i)G(s,i)\right),$$

where $F(s,i) = b(1-s) + (d-\beta)si$, $G(s,i) = (p-q)\beta si + (d-q\beta)i^2 + (q\beta - b - d)i$ and $H(s,i) = \frac{1}{i}$. The proposition statement holds by Dulac's negative criterion provided that $q > \frac{d}{\beta}$. □

The existence of periodic solutions for some $q < \frac{d}{\beta}$ is not theoretically outlawed. However, the system (3) can not undergo a Hopf bifurcation since, whenever the enzootic equilibrium (s^*, i^*) exists, we always have $Tr(J(s^*, i^*)) > 0$ and $det(J(s^*, i^*) > 0$. Therefore, if periodic solutions exist, they must arise far from the equilibrium (s^*, i^*), yet still containing it in their interior. Intensive numerical search uncovered no such special solutions and strongly suggest the global stability of the enzootic equilibrium even in this case. We leave this problem for a future investigation.

Received on January 1, 2008. Accepted on April 23, 2008.

E-mail address: dobromir@scharp.org
E-mail address: kingaa@umich.edu